Propulsion and Power Research 2013;2(2):131–138

http://ppr.buaa.edu.cn/

Propulsion and Power Research

www.sciencedirect.com

ORIGINAL ARTICLE

The development and application of an inviscid inverse method

Jinguang Yang*, **Hu Wu**

School of Power and Energy, Northwestern Polytechnical University, Xi'an 710072, China

Received 16 December 2012; accepted 22 January 2013
Available online 22 May 2013

KEYWORDS

Inverse method;
Pressure loading;
Aerodynamic design;
Turbomachinery

Abstract A two-dimensional inviscid inverse method is developed, verified and applied in this paper. The method solves the Euler equation in absolute reference frame by a cell-centered finite volume method, and the hybrid Runge-Kutta method is used for time integration. Different from the direct method, the inverse method imposes a unique "transpiration" boundary condition on the blade surfaces. The inputs of inverse method are pressure loading and blade tangential thickness distribution along the blade chord. During the time marching process, the blade shape is periodically updated. When the solution is converged, the blade shape will be stabled. In the paper, the principle of the inverse method is described in detail. Then the developed inverse method is verified against a consistence test: recover an axial compressor cascade from a different start. Finally, to demonstrate the powerful capability of the method, it is used to redesign the cascade, and final results give an improved aerodynamic performance.

1. Introduction

Compressors and turbines are key components of gas turbine engines, and their design methods largely determine the aerodynamic performance and economy of the propulsion system. Traditionally two-dimensional/quasi-three-dimensional (2D/quasi-3D) axi-symmetric through-flow based design systems had been matured for a long time and were still widely used in modern turbomachinery design practice. However, much endeavor towards a full

*Corresponding author: Tel.: +86 29 88492744.
E-mail address: jinguang_yang@126.com (Jinguang Yang).

Peer review under responsibility of National Laboratory for Aeronautics and Astronautics, China.

Production and hosting by Elsevier

2212-540X © 2013 National Laboratory for Aeronautics and Astronautics. Production and hosting by Elsevier B.V. All rights reserved.
http://dx.doi.org/10.1016/j.jppr.2013.04.005

Nomenclature

E	total internal energy
$\boldsymbol{F}$	axial flux
$\boldsymbol{G}$	tangential flux
H	total enthalpy
T	static temperature
$\boldsymbol{U}$	conservative vector
V_x	axial velocity
V_y	tangential (y direction in 2D) velocity
V_{mov}	blade translation velocity
W_x	relative axial velocity
W_y	relative tangential velocity
f	camber line y coordinates
p	static pressure
x	axial coordinates
y	tangential coordinates
α	blade surfaces
ρ	fluid density
Δp	pressure loading

Superscripts

*	target value
m	iteration counter

three-dimensional design system has been made. The rapid development of computational fluid dynamics (CFD) techniques and the increasingly strong computational power make a three-dimensional direct simulation become a standard design process of turbomachines. But there is still a long way to go for the truly three-dimensional design system to be used commonly as its analysis counterpart.

In aerodynamic field of turbomachinery, most of the problems can be summarized into two problems: analysis problem (direct mode) and design problem (inverse mode). Knowing the geometry and computing its performance lend itself to the analysis problem, and specifying the performance and trying to obtain the geometry belong to the inverse problem. The turbomachinery aerodynamic design problem is the inverse problem in nature, and relative methods are termed as inverse method.

Till now, the inverse design technique, involving CFD technique, can be classified into 4 classes, namely the numerical optimization based inverse method, the hybrid inverse method, the direct-mode based inverse method, and pure inverse method. Concerning the numerical optimization based inverse method [1], it involves optimization technique to determine the new blade shape, as shown in Figure 1. Although optimization might find an optimized solution, it usually needs very large computing sources; also most optimization methods can only obtain a local optimum value. As shown in Figure 2, Demeulenaere et al. had proposed a hybrid inverse method [2,3], which incorporates an analysis flow solver and an inverse flow solver together, the analysis solver is used to calculate the flow-field, and the inverse one is used to obtain the new blade shape. Another type of the inverse method is a little easier, it only utilizes an analysis flow solver to predict the flow, and then changes the blade shape according to the differences of computed parameters with specified ones, such application includes references [4–6] etc. All of three above-mentioned inverse methods shared a common feature: they all involve the direct flow solver. Dang et al. [7–9] devised a novel inverse method, which only involves an inverse flow solver, as shown in Figure 4. In the method, the specified parameters are enforced by inverse boundary condition (BC), so the computational time of such an inverse solution is basically comparable to a direct flow analysis. The work of Ahmadi and Ghaly [10], Tiow and Zangeneh [11], and Qiu, Ji and Dang [12] belong to this category. Due to its short computing time, easy implementation and applicapable to all types of turbomachines, the method is adopted in present study.

In this paper, a two-dimensional inverse method is developed based on the specified pressure loading and blade pitch-wise thickness. The selected specified parameters not only enable a good control over performance (mass-averaged swirl, pressure ratio, mass flow rate etc), but also easily ensure structure integrity. The proposed method solves Euler equations together with a mass transpiration model on the blade surface, and the camber line of the blade is generated according to the so called "flow tangency" condition. The inverse mode of the solver

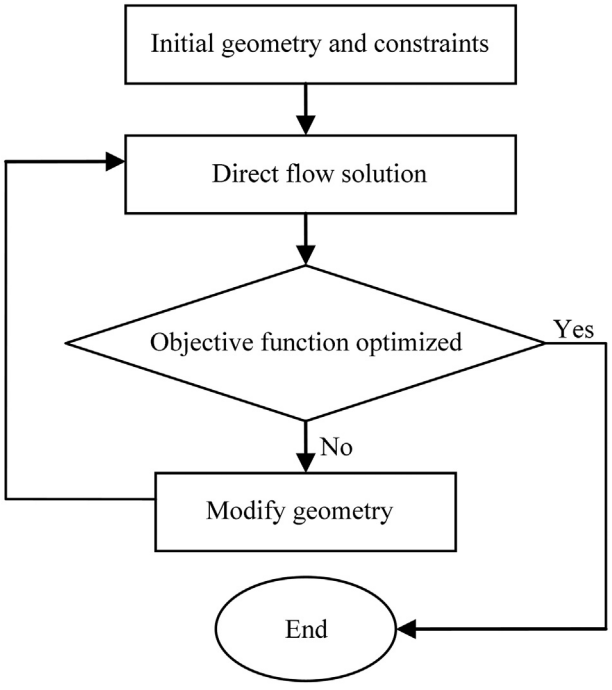

Figure 1 Numerical optimization based inverse method.

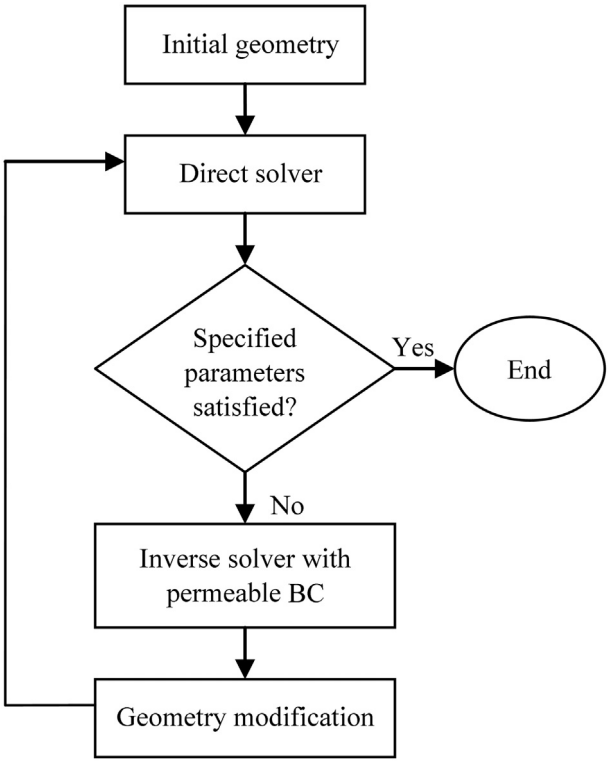

Figure 2 Hybrid inverse method.

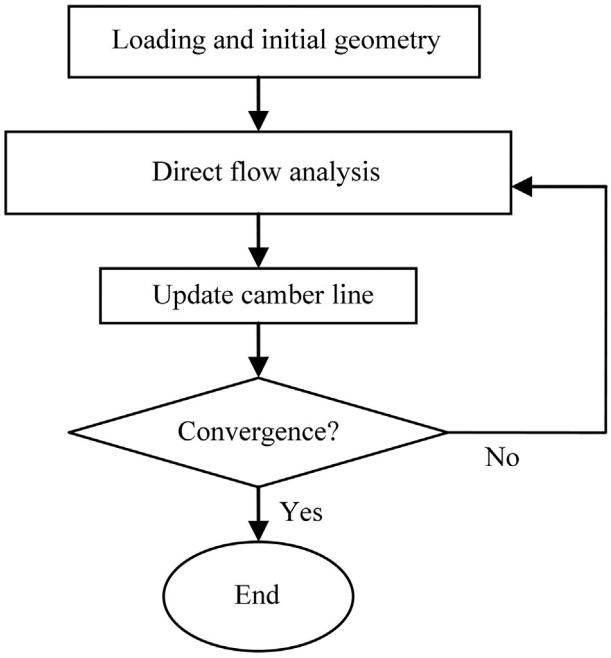

Figure 3 Direct mode based inverse method.

is validated against the 2D profile of Deutsches Zentrum für Luft- und Raumfahrt (DLR) rotor cascade [13]. At last, the method is used to redesign the cascade in order to improve its adiabatic efficiency.

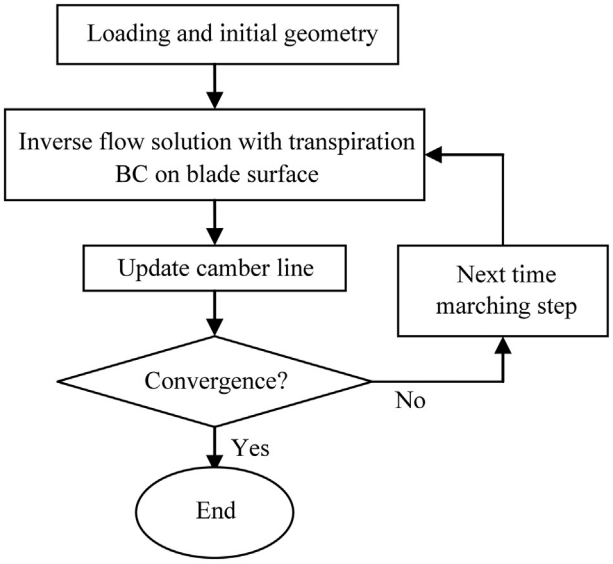

Figure 4 Pure inverse method.

2. Flow solver

Two-dimensional Euler equations in an absolute reference frame are solved here, namely

$$\frac{\partial \boldsymbol{U}}{\partial t}+\frac{\partial \boldsymbol{F}}{\partial x}+\frac{\partial(\boldsymbol{G}-V_{mov}\boldsymbol{U})}{\partial y}=0 \tag{1}$$

where $\boldsymbol{U}$ is the conservative variables vector, defined as

$$\boldsymbol{U}=(\rho,\rho V_x,\rho V_y,\rho E)^{\mathrm{T}}$$

and the flux vectors $\boldsymbol{F}$ and $\boldsymbol{G}$ are defined as

$$\boldsymbol{F}=(\rho V_x,\rho V_x^2+p,\rho V_x V_y,\rho H V_x)^{\mathrm{T}}$$

$$\boldsymbol{G}=(\rho V_y,\rho V_y V_x,\rho V_y^2+p,\rho H V_y)^{\mathrm{T}}$$

V_{mov} is the translational velocity in y direction, and E is total internal energy, and H is the total enthalpy, they can be computed as

$$E=c_v T+\frac{1}{2}(V_x^2+V_y^2),\quad H=E+p/\rho.$$

With supplemented the equation of status for the perfect gas, now the equation system is closed.

The equation is discretized by a cell-centered finite volume method, and the robust Jameson-Schmidt-Turkel scheme [14] is used here, it is a central difference scheme plus a 1st and 3rd order artificial viscosity. A five-stage hybrid Runge-Kutta method integrates the semi-discretized equation in time direction. In order to accelerate the convergence, two measurements are adopted in the code, namely the local time step technique and the implicit residual smoothing.

The grid used here is of a simple-H type structured grid, or may be called as a shear-H grid. Although some more sophisticated grid generation techniques are available, past experience shows that this simple-H type grid can achieve a

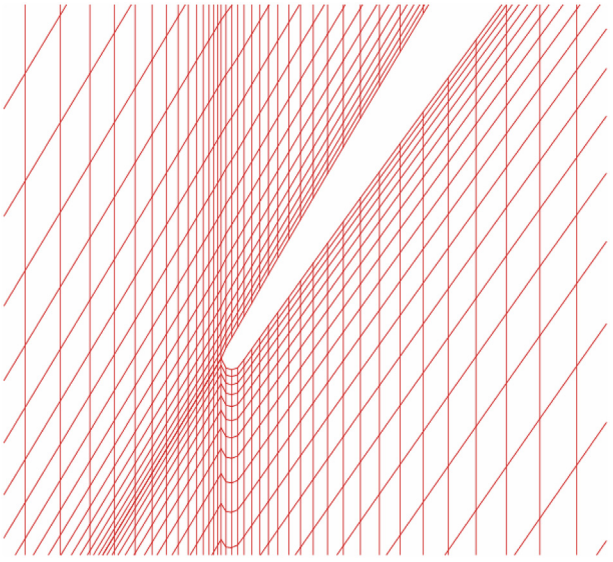

Figure 5 Typical simple-H grid around the leading edge of the DLR rotor cascade.

good compromise between the grid quality and easy grid generation, also facilitate the implementation of the inverse method developed in the paper. Figure 5 shows a typical grid around the leading edge of a compressor cascade.

Four types of boundary conditions are available in the code; they are the subsonic inlet, the subsonic outlet, the solid wall and periodic boundary condition. At inlet, total temperature, total pressure and flow angle are specified and static pressure is extrapolated from physical domain. At outlet, static pressure is specified, and all of the other three variables are extrapolate form interior. No-flux boundary condition is imposed at blade surface for analysis mode, and wall function is used [15], which allows a much coarser grid. Direct copy from cells in adjacent blade passage is used to properly impose the periodic boundary condition.

3. Inverse method

3.1. Basic theory

The inverse mode differs from the direct one mainly in the blade surface boundary conditions. For the direct mode, the blade surfaces are treated as solid walls, exactly as those for the hub and casing walls. But for the inverse mode, a "mass transpiration" model is used, which allows mass to flow through this "solid wall" during the iteration process. When the solution converges, the flow will align with the blade surface, and no mass flow penetration is resumed. The formulation of this inverse boundary condition is derived according to "flow tangency condition" as follows,

$$W^{\pm}\cdot\nabla\alpha^{\pm}=0 \tag{2}$$

where $W^{\pm}$ represents the relative velocity on the suction and pressure surfaces, and $\nabla\alpha^{\pm}$ symbols the unit normal vector of the blade surfaces, as shown in Figure 6.

According to Figure 6, relative position of blade surface with respect to the camber line is defined as

$$\alpha^{\pm}\equiv y-\left(f\pm\frac{t}{2}\right)=n\tau \tag{3}$$

where $f=f(x)$ is the mean camber line, $t=t(x)$ is the tangential thickness and n is the blade number.

Substituting Eq. (3) into Eq. (2) yields the following tangential condition expression:

$$-W_x^{+}\left(\frac{\mathrm{d}f}{\mathrm{d}x}+\frac{1}{2}\frac{\mathrm{d}t}{\mathrm{d}r}\right)+W_y^{+}=0 \tag{4}$$

for the upper surface and

$$-W_x^{-}\left(\frac{\mathrm{d}f}{\mathrm{d}x}-\frac{1}{2}\frac{\mathrm{d}t}{\mathrm{d}r}\right)+W_y^{-}=0 \tag{5}$$

for the lower surface.

By considering

$$W_x=V_x,\quad W_y=V_y-V_{mov} \tag{6}$$

the flow tangential condition could be expressed by absolute variables

$$-V_x^{+}\left(\frac{\mathrm{d}f}{\mathrm{d}x}+\frac{1}{2}\frac{\mathrm{d}t}{\mathrm{d}x}\right)+V_y^{+}-V_{mov}=0 \tag{7}$$

$$-V_x^{-}\left(\frac{\mathrm{d}f}{\mathrm{d}x}-\frac{1}{2}\frac{\mathrm{d}t}{\mathrm{d}x}\right)+V_y^{-}-V_{mov}=0 \tag{8}$$

Adding and subtracting Eq. (7) and Eq. (8) respectively gives

$$V_{x,bl}\frac{\mathrm{d}f}{\mathrm{d}x}=V_{y,bl}-V_{mov}-\frac{1}{4}\frac{\mathrm{d}t}{\mathrm{d}x}\Delta V_x \tag{9}$$

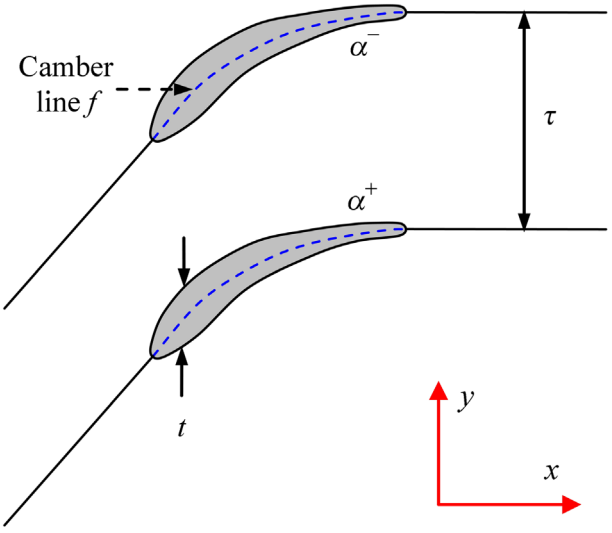

Figure 6 Blade cascade configuration.

$$\Delta V_y = \Delta V_x \frac{\mathrm{d}f}{\mathrm{d}x} + V_{x,bl} \frac{\mathrm{d}t}{\mathrm{d}x} \tag{10}$$

the subscript "*bl*" means the blade value, taking V_y as example,

$$V_{y,bl} = \frac{1}{2}(V_y^+ + V_y^-) \tag{11}$$

and the "Δ" operator is defined as

$$\Delta V_y = V_y^+ - V_y^- \tag{12}$$

For the transpiration model, the inverse boundary condition must ensure the pressure loading which is specified as the design intent, so the static pressure is updated as follows

$$(p^{\pm})^{m+1} = (p_{bl})^m \pm \frac{1}{2}\Delta p^* \tag{13}$$

where the superscript "*" refers to the target value, m is the index of the last time step, and m+1 is the index of current time step. The tangential condition is partially imposed by setting the tangential velocities as

$$(V_y^{\pm})^{m+1} = (V_{y,bl})^m \pm \frac{1}{2}\Delta V_y \tag{14}$$

where ΔV_y is computed by Eq. (12).

For the inverse method, at every iteration step, the camber line will be regenerated so as to meet the flow tangential condition as much as possible. Then the given tangential thickness is superimposed to construct the cascade. Equation (10) is taken as the camber line updating equation and it can be integrated using the trapezoidal method.

As mentioned above, the flow tangential condition is not strictly enforced in the inverse boundary conditions, so there will be the mass flux across the blade surfaces during iterations, which is different from the direct mode. However, the camber line generation equation is served to align the blade with the flow, so when the inverse method is converged, the flow tangential condition and the zero-mass-flux condition is automatically satisfied. The other variables for the inverse boundary conditions are treated in the same way as those for the direct mode.

For the simple H-type grid, the grids of the same streamwise index (I) on both blade surfaces share the same x coordinate. This facilitates the implementation of the inverse method, so is the grid generation. When the camber line is regenerated, the grid has to be regenerated too. In order to lower the relative computation time, an algebraic stretching function is specified and used in the grid generation process.

3.2. Design process

The inverse design process is illustrated in Figure 4. The essential steps include:

(1) read in input data, including initial geometry data, specified pressure loading and thickness distribution etc;
(2) perform flow computation in the inverse mode;
(3) compute the new blade camber line, then the new blade shape, regenerate the grid and re-calculate the metrics;
(4) check solution convergence. If converged, post-process is conducted; if not, go back to step (2) for a new iteration.

The convergence criterion is defined by the flow field residual and the relative change of blade shape. Here the flow is considered to be converged when the error of the continuity equation is driven down to 5 orders, and the relative change of blade camber normalized by the axial chord is lower than 1×10^{-5}.

4. Results

4.1. Inverse mode verification

The validity of the inverse model is verified through a "consistence test", which should recover the original profile shape from different start geometry. The test case used here is a 2D cascade extracted from the DLR rotor [13]. Figure 7 shows the specified pressure loading. The accuracy of current inverse method could be demonstrated from Figure 8, which shows the geometry change. The starting geometry is obtained by linearly shifting the original blade from leading edge (LE) to trailing edge (TE), the displacement at the TE position is about 2% of the axial chord, so the start geometry is very different from the target one. However, the final profile computed by the inverse method is fairly close to the target, only with minor discrepancies at the LE and TE position. The error can be attributed to geometry modeling error induced by the simple-H type grid. Figure 9 compares the direct and inverse calculated relative Mach number contours for the direct and inverse calculations, which are used to demonstrate the "consistence" of the flow filed. The solid line is the result computed in the direct mode, and dashed one is inversely computed. As shown in Figure 9, the overall consistence is very good. For the DLR rotor 2D

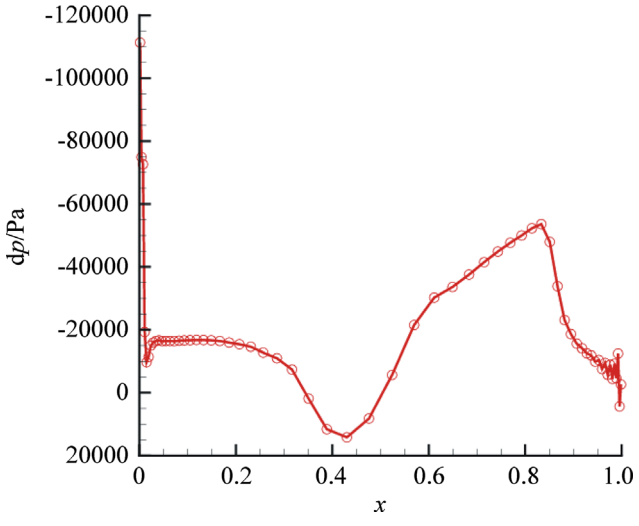

Figure 7 Specified loading distributione for the consistence test of DLR cascade.

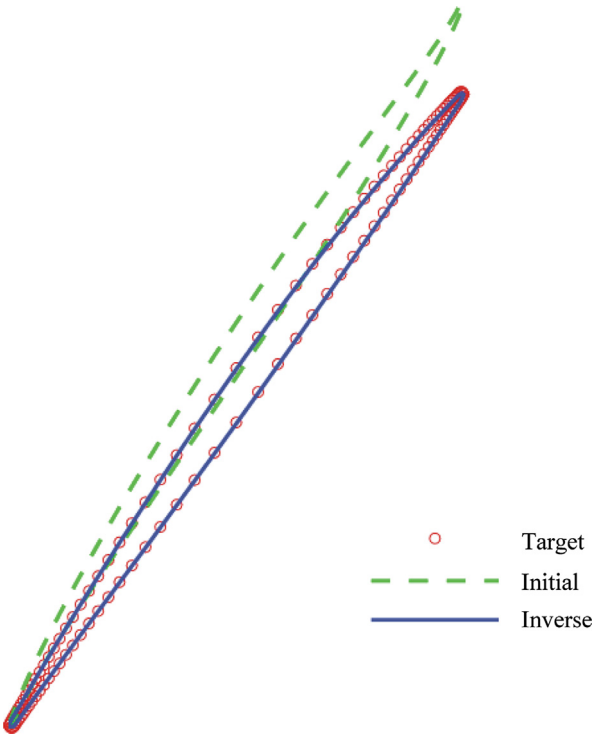

Figure 8 Geometric comparison for the consistence test of DLR cascade.

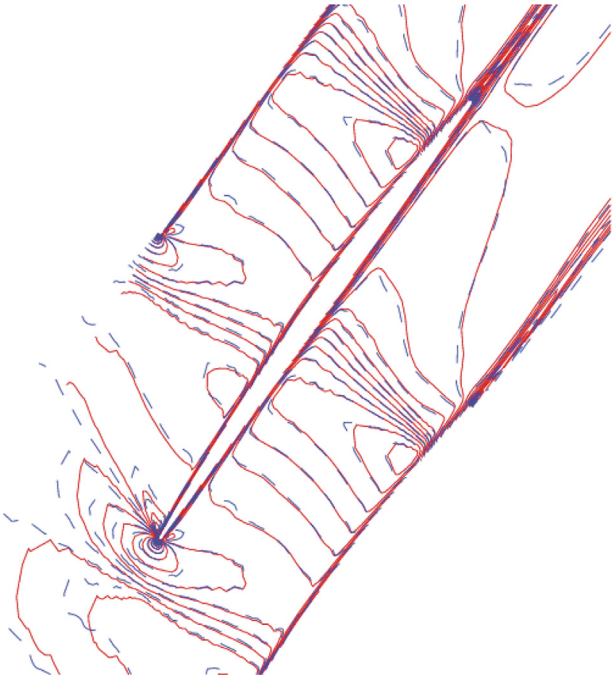

Figure 9 Mach number comparison for the consistence test of DLR cascade.

cascade test case, Figure 10 gives the convergence history of the flow filed residual and the camber line geometry error, which could indicate the efficiency of the current inverse method. The camber line error is non-dimensionalized by the axial chord. For the case considered here, the inverse method is converged after

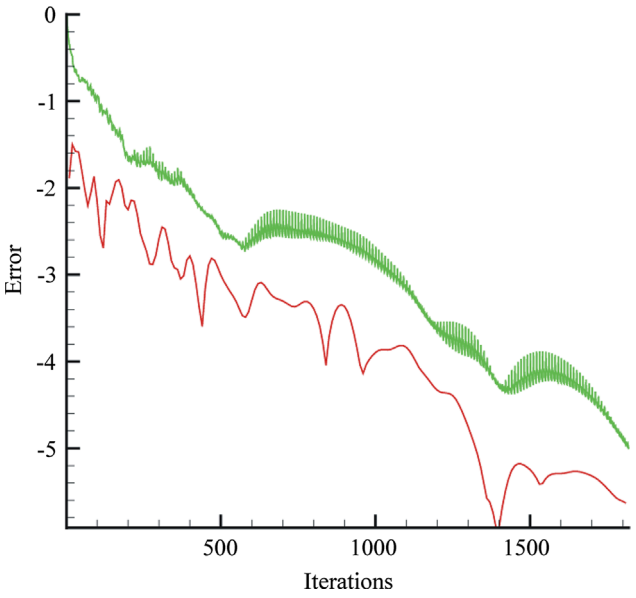

Figure 10 Convergence history for the consistence test of DLR cascade.

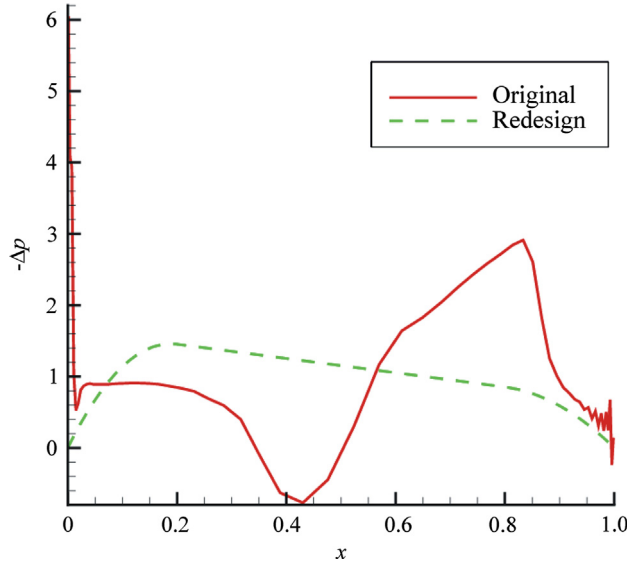

Figure 11 Loading distribution for the redesign of the DLR cascade.

1819 iterations, which means the flow error is less than 1×10^{-5}, so is the camber line error. During the calculation, the camber line is updated every 10 time steps, that explains why there are small spikes in Figure 10.

Based on the above-mentioned facts, it may be concluded that the developed inverse mode can accurately recover the geometry and the flow field.

4.2. Redesign of the 2D cascade

After verifying the developed inverse method, it's used to redesign the 2D DLR rotor cascade. As shown in Figure 8, the loading of original cascade posses the following features: (1) there is a large loading spike at the LE

position, which is caused by the leading edge circle; (2) the first detached shock causes negative loading at approximately 40% axial chord location; (3) the passage normal shock made the loading drop dramatically, and induces a thick wake. In order to eliminate these undesirable flow phenomena, the redesigned loading is specified as the dashed line in Figure 11, which imposing an unloaded leading edge, a forward-loaded and smooth loading profile, and an unloaded trailing edge to satisfying the Kutta condition. It's expected the redesign case can obtain a higher efficiency at the same pressure ratio and mass flow rate.

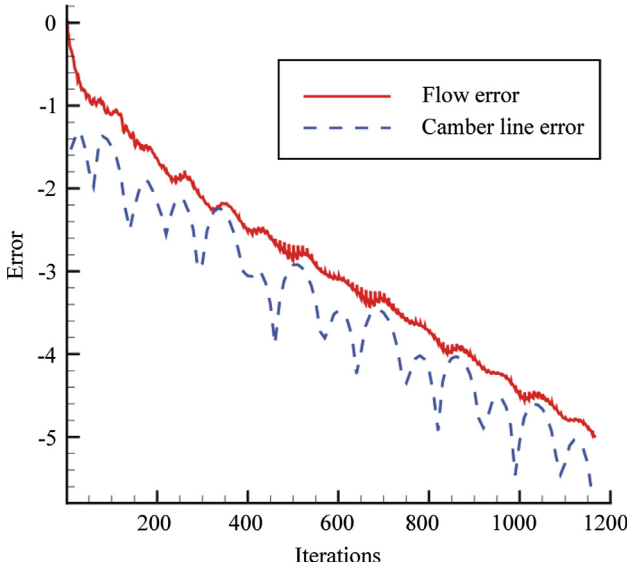

Figure 12 Convergence history for the redesign of the DLR cascade.

Table 1 Overall performance comparison for the original and redesigned cascade.

	Original	Redesigned
Mass flow/(kg/s)	5.925	5.981
Total pressure ratio	1.3825	1.3850
Efficiency	0.9268	0.9596

During the time marching process, the blade shape is updated every 10 time steps, and an under-relaxation factor, typically 0.2, is used for the camber line position to make the calculation stable. The inverse computation is considered to be converged after about 1150 time steps, the convergence history is shown is Figure 12. The overall performance for the original and redesigned case is compared in Table 1. It's obvious that there is a more than 3 points efficiency gain at the basically the same mass flow and total pressure ratio, which demonstrates the function of the developed inverse method.

The blade shapes of the original and redesigned geometry are plotted in Figure 13. According to these results, it's found that the camber line near the LE of the redesigned blade is shift upward, which forms a sharper LE shape. It's well known that a shape LE is more suited to the local supersonic flow. So sharp LE is impossible for practical use, but here it does reflect the design intent—eliminate large pressure loading spike caused by the LE circle. At the rear part of the blade, the camber line is shifted downward, making the blade "de-cambered", so a better performance can be achieved. From the Mach number contour shown in Figure 14(a), the influence of geometry change on flow filed can be fully understood. Comparing to the two-shock configuration, the redesigned one only has one detached shock, with basically the same shock-front Mach number as the passage normal shock of the original one. Also the detached shock impinges the suction side with a slope. This will significantly reduce the shock loss and related profile loss. Figure 14(b) plots the entropy contour. It's apparent that the redesigned one has a thinner wake. Those explain where the performance gain originates.

5. Conclusions

In this paper, a two-dimensional inviscid inverse method is developed and validated. Then the method is used to redesign a compressor cascade with shocks. The results demonstrate that the developed method is feasible for design cases with supersonic flow and shock. Also the method enables the designer a more direct control over the aerodynamic performance of turbomachines under certain

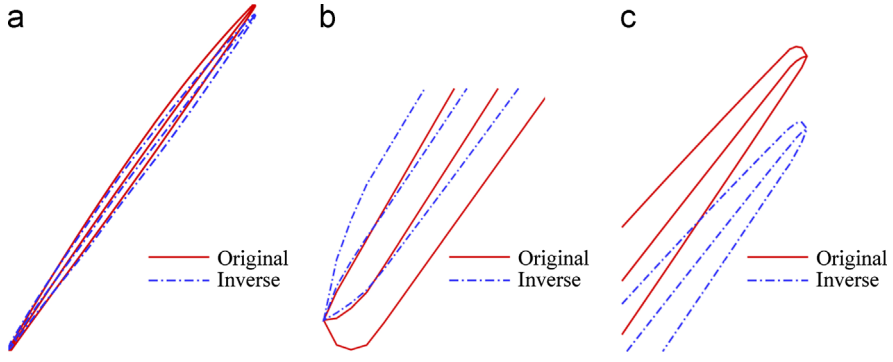

Figure 13 Comprison of blade shape. (a) Overall geometry comparison, (b) leading edge detail and (c) trailing edge detail.

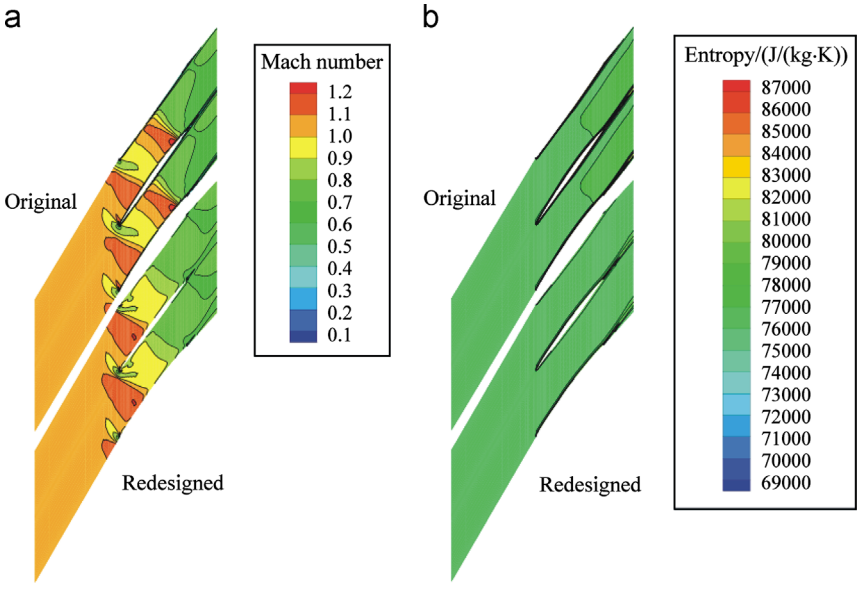

Figure 14 Flowfield comprison for the original and redesigned cascade. (a) Mach number contour and (b) entropy contour.

constraints (mass flow rate, total pressure ratio etc). The present method is easily extended to three dimensions and this will be done in the further investigations.

Acknowledgements

The author would like to thank the support of National Science Foundation of China (Grant No. 51076131) for supporting the present research.

References

[1] S. Burguburu, C. Toussaint, C. Bonhomme, G. Leroy, Numerical optimization of turbomachinery bladings, ASME Journal of Turbomachinery 126 (1) (2004) 91–100.
[2] A. Demeulenaere, R. Van den Braembusche, Three-dimensional inverse method for turbomachinery blading design, Journal of Turbomachinery 120 (2) (1998) 247–255.
[3] O. Leónard, R. Van den Braembussche, Two-dimensional transonic aerodynamic design method, ASME Journal of Turbomachinery 114 (3) (1996) 553–560.
[4] J.E. Borges, L.M.C. Gato, R.M.R.J. Pereirat, Iterative use of a time-marching code for designing turbomachine blade rows, Computers & Fluids 25 (2) (1996) 197–216.
[5] J.C. Páscoa, A.C. Mendes, L.M.C. Gato, A fast iterative inverse method for turbomachinery blade design, Mechanics Research Communications 36 (5) (2009) 630–637.
[6] W.T. Tiow, K.F.C. Yiu, M. Zangeneh, Application of simulated annealing to inverse design of transonic turbomachinery cascades, Proceedings of the Institution of Mechanical Engineers, Part A: Journal of Power and Energy 216 (1) (2002) 59–73.
[7] T. Dang, Inverse method for turbomachine blades using shock-capturing techniques, AIAA Paper 95-2465, 1995.
[8] T. Dang, V. Isgro, Euler-based inverse method for turbomachine blades, part 1: two-dimensional cascades, AIAA Journal 33 (12) (1995) 2309–2315.
[9] T. Dang, S. Damle, X. Qiu, Euler-based inverse method for turbomachines blades, part 2: three-dimensional flows, AIAA Journal 38 (11) (2000) 2007–2013.
[10] M. Ahmadi, W.S. Ghaly, Aerodynamic inverse design of turbomachinery cascades using a finite volume method on unstructured meshes, Inverse Problems in Science and Engineering 6 (4) (1998) 281–298.
[11] W.T. Tiow, M. Zangeneh, Applicatoin of a three-dimensional viscous transonic inverse method to NASA rotor 67, Proceedings of the Institution of Mechanical Engineers, Part A: Journal of Power and Energy 216 (3) (2002) 243–255.
[12] X. Qiu, M. Ji, T. Dang, Three-dimensional viscous inverse method for axial blade design, Inverse Problems in Science and Engineering 17 (8) (2009) 1019–1036.
[13] L. Fontter, Test cases for computational of internal flows in aero engine components, AGARD AR-275 (1990).
[14] A. Jameson, W. Schmidt, E. Turkel, Numerical solutions of the Euler equations by finite volume methods using Runge-Kutta time-stepping schemes, AIAA Paper 81-1259, 1981.
[15] J. Denton, The calculation of three-dimensional viscous flow through multistage turbomachines, Journal of Turbomachinery 114 (1) (1992) 18–26.